Recent progress in the NSTX/NSTX-U lithium programme and prospects for reactor-relevant liquid-lithium based divertor development

2013 Nucl. Fusion 53 113030

(http://iopscience.iop.org/0029-5515/53/11/113030)

Nucl. Fusion **53** (2013) 113030 (11pp) doi:10.1088/0029-5515/53/11/113030

Recent progress in the NSTX/NSTX-U lithium programme and prospects for reactor-relevant liquid-lithium based divertor development

M. Ono[1], M.A. Jaworski[1], R. Kaita[1], H.W. Kugel[1], J.-W. Ahn[2], J.P. Allain[3], M.G. Bell[1], R.E. Bell[1], D.J. Clayton[4], J.M. Canik[2], S. Ding[5], S. Gerhardt[1], T.K. Gray[2], W. Guttenfelder[1], Y. Hirooka[6], J. Kallman[1,7], S. Kaye[1], D. Kumar[4], B.P. LeBlanc[1], R. Maingi[2], D.K. Mansfield[1], A. McLean[2,7], J. Menard[1], D. Mueller[1], R. Nygren[8], S. Paul[1], M. Podesta[1], R. Raman[9], Y. Ren[1], S. Sabbagh[10], F. Scotti[1], C.H. Skinner[1], V. Soukhanovskii[7], V. Surla[11], C.N. Taylor[3], J. Timberlake[1], L.E. Zakharov[1] and the NSTX Research Team

[1] Princeton Plasma Physics Laboratory, PO Box 451, Princeton, NJ 08543, USA
[2] Oak Ridge National Laboratory, PO Box 2008, Oak Ridge, TN 37831, USA
[3] College of Engineering, Purdue University, West Lafayette, IN 47907, USA
[4] Physics and Astronomy, Johns Hopkins University, Baltimore, MD 21218, USA
[5] Academy of Science Institute of Plasma Physics, Hefei, People's Republic of China
[6] National Institute for Fusion Science, 322–6 Oroshi, Toki, Gifu 509–5292, Japan
[7] Lawrence Livermore National Laboratory, Livermore, CA 94551, USA
[8] Sandia National Laboratory, Albuquerque, NM 87185, USA
[9] Department of Aeronautics and Astronautics, University of Washington at Seattle, Seattle, WA 98195, USA
[10] Department of Applied Physics, Columbia University, New York, NY 10027, USA
[11] Center for Plasma-Materials Interactions, University of Illinois, Urbana-Champaign, IL, USA

E-mail: mono@pppl.gov

Received 7 January 2013, accepted for publication 3 October 2013
Published 24 October 2013
Online at stacks.iop.org/NF/53/113030

Abstract
Developing a reactor-compatible divertor has been identified as a particularly challenging technology problem for magnetic confinement fusion. Application of lithium (Li) in NSTX resulted in improved H-mode confinement, H-mode power threshold reduction, and other plasma performance benefits. During the 2010 NSTX campaign, application of a relatively modest amount of Li (300 mg prior to the discharge) resulted in a ~50% reduction in heat load on the liquid lithium divertor (LLD) attributable to enhanced divertor bolometric radiation. These promising Li results in NSTX and related modelling calculations motivated the radiative LLD concept proposed here. Li is evaporated from the liquid lithium (LL) coated divertor strike-point surface due to the intense heat flux. The evaporated Li is readily ionized by the plasma due to its low ionization energy, and the poor Li particle confinement near the divertor plate enables ionized Li ions to radiate strongly, resulting in a significant reduction in the divertor heat flux. This radiative process has the desired effect of spreading the localized divertor heat load to the rest of the divertor chamber wall surfaces, facilitating the divertor heat removal. The LL coating of divertor surfaces can also provide a 'sacrificial' protective layer to protect the substrate solid material from transient high heat flux such as the ones caused by the edge localized modes. By operating at lower temperature than the first wall, the LL covered large divertor chamber wall surfaces can serve as an effective particle pump for the entire reactor chamber, as impurities generally migrate towards lower temperature LL divertor surfaces. To maintain the LL purity, a closed LL loop system with a modest circulating capacity (e.g., ~1 l s^{-1} for ~1% level 'impurities') is envisioned for a steady-state 1 GW-electric class fusion power plant.

(Some figures may appear in colour only in the online journal)

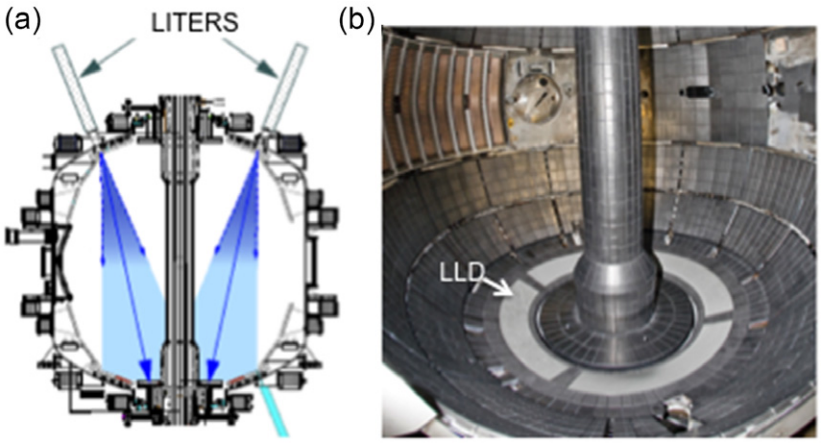

Figure 1. (*a*) Schematic of dual Li evaporator set-up. (*b*) Liquid Li divertor in NSTX.

1. Introduction

Developing a reactor-compatible divertor is a particularly challenging physics and technology problem for magnetic confinement fusion [1, 2]. While tungsten has been identified as the most attractive solid divertor material, many challenges including surface cracking and deleterious modification of the surfaces by the plasma must be overcome to develop robust plasma-facing components (PFCs) [3]. In recent DEMO divertor design studies [4–6], the steady-state heat handling capability of a tungsten-based divertor design is only about 5–10 MW m^{-2} which is nearly an order of magnitude lower than the anticipated heat flux ∼40–60 MW m^{-2} for the next generation ST-based Fusion Nuclear Science Facility (FNSF) [7], Pilot Plant [8], and a 1 GW-electric-class DEMO/Power Plant with the device size of ITER. In addition, there are serious concerns over potential deterioration and damage to the plasma-facing surfaces by the very high heat fluxes accompanying edge localized mode (ELMs) and other transient events. Clearly it is highly desirable to formulate a DEMO-relevant divertor concept, which can handle the high steady-state divertor heat flux and also survive the transient events.

In this paper, we investigate a liquid-lithium (LL) based radiative divertor concept which we term RLLD (radiative liquid-lithium divertor) in order to solve the challenging divertor heat load issues for future devices including FNSF, Pilot Plant and Demo. It should be noted that the lithium (Li) PFC research in magnetic fusion experiments has started on TFTR in 1990s following the discovery that lithium coating of the graphite PFCs improved plasma confinement and fusion performance [9]. With encouraging experimental results in TFTR, the APEX study was initiated to encourage innovation and scientific understanding for Li-based fusion PFCs [10]. Since then, the benefits of Li have been experimentally verified in a growing number of magnetic confinement fusion devices worldwide [11–19]. Summary reports on the recent symposiums on Li research can be seen in [20, 21]. In this paper, a summary of Li experiments conducted in the National Spherical Torus Experiment (NSTX) [22] relevant for the present paper is given in section 2. In section 3, in order to understand the divertor heat load reduction observed in NSTX with Li PFC coating, a simple Li divertor radiative model calculation is described. The model predicts reductions in the heat flux to the divertor by localized lithium radiation which appears to be consistent with measurements made in NSTX. Encouragingly, even for an ITER-size 1 GW-electric fusion power plant, the calculated required Li evaporation rate is quite modest. In section 4, an example of RLLD concept is presented and we examine the compatibility of the RLLD system in a fusion reactor environment. In section 5, the conclusions and discussions are given.

2. NSTX lithium experimental overview

Various Li wall coating techniques have been experimentally explored on NSTX since 2006. A major accomplishment of the NSTX Li research is the demonstration of the H-mode plasma performance improvements with Li for the first time [23]. The Li experimentation on NSTX started with a few milligrams of Li pellets injected into the plasma, and it has evolved to a dual Li evaporation system (LITER) which can evaporate up to ∼160 g of Li onto the lower divertor plates between re-loadings as shown in figure 1(*a*). The LITER system is described in [23]. In 2010, the NSTX Li research has focused on the effect of LLD surface on the divertor as shown in figure 1(*b*) [24]. The LLD plate is a copper substrate with a thin (∼0.2 mm thick) stainless steel layer covered by a ∼50% porous molybdenum coating to promote uniform Li coating by capillary action. With the dual LITER system, 1300 g of Li was evaporated into the NSTX vacuum vessel during the 2010 operations. The Li deposited on the LLD was about twice the amount needed to fill its porous molybdenum surface. The application of Li coating on NSTX has yielded a significant improvement in the electron confinement with Li coating of carbon tiles in H-mode plasmas. Similar H-mode confinement and plasma performance improvements with lithium divertor coating have been observed with LLD as well.

A comparison of Li and non-Li coated otherwise similar neutral beam injection (NBI) heated deuterium H-mode discharges is shown in figure 2(*a*) [16, 23]. Importantly, the Li evaporation resulted in a broadening of H-mode electron temperature profile compared to the one without Li application for similar integrated plasma densities as shown

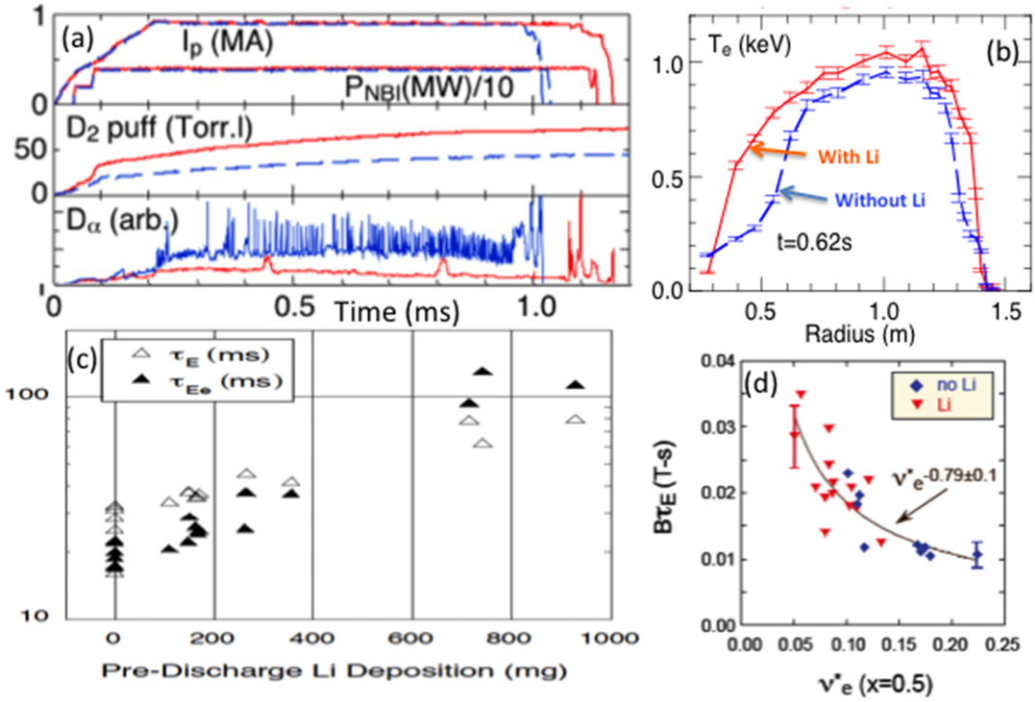

Figure 2. Plasma performance improvements with Li in NBI heated H-mode discharges. (*a*) Plasma discharge traces with and without Li in NSTX. Red traces are with Li and blue-dashed traces are without Li. (*b*) Electron temperature profiles with Li (red) and without Li (blue-dashed). (*c*) Total and electron energy confinement time (τ_E and τ_{Ee}, respectively) versus pre-discharge Li evaporation amount. (*d*) Normalized energy confinement time versus electron collisionality and without Li as labelled.

in figure 2(*b*) [25]. The broadened electron temperature significantly increased the electron stored energy and therefore the electron energy confinement time. Also the broadening of the electron temperature broadens the plasma pressure profile resulted in improved plasma MHD stability at high beta beneficial for advanced plasma operations. While significant ion energy confinement improvement was not observed with Li, the ion energy transport in the NSTX H-mode plasma is already comparable to the neoclassical values so the result is not surprising. In terms of particle pumping, as shown in figure 2(*a*), the Li application significantly decreases the D_α signal, which is a measure of the edge recycling of deuterium gas. The reduction in recycling is achieved with Li even though nearly twice as much deuterium gas was injected to maintain similar plasma density. This demonstrates that the Li coating can absorb (pump) impinging deuterium ions and atoms. Also evident in the figure, the ELM activity is greatly reduced with Li and often ELMs are completely supressed. This ELM stabilization is attributed to the localized edge density reduction and resulting broadening of the edge pressure gradient near the H-mode pedestal [26]. Thus far, the electron energy confinement continues to improve with the amount of Li evaporated without reaching an apparent saturation, which suggests that further improvements may be possible as shown in figure 2(*c*) [27]. Analysis with the TRANSP code indicates that the electron thermal diffusivity in outer region is progressively reduced with increasing Li evaporation. It is interesting to note that the improving electron energy confinement with Li is consistent with the trend of improved electron energy confinement with reduced collisionality generally observed in NSTX as shown in figure 2(*d*) where normalized energy confinement time was plotted as a function of collisionality for both lithium and non-lithium discharges [28]. The improved electron energy confinement with lower collisionality is attributed to the stabilization of microtearing modes in the recent theoretical modelling work [29] but this model while promising is not yet confirmed experimentally. Additionally, Li was shown to reduce the H-mode power threshold [30]. NSTX Li experiments have also produced an enhanced pedestal H-mode with significantly improved energy confinement with $H_{\text{ITER-98}}$ up to 1.7 [31]. This degree of H-mode confinement improvement should enable a compact ST-based fusion system such as the FNSF and Pilot Plants [7, 8] which typically requires $H_{\text{ITER-98}}$ of 1.3–1.6. The Li PFC is therefore a highly promising tool to improve H-mode performance and eventually to enhance fusion power plant performance.

It is also noted that even with significant applications of Li on PFCs, Li ion fraction in main fusion plasma core remains very low ($\leqslant$0.05%) even during H-modes as shown in figure 3(*a*) [32]. There are a number of contributing factors for the observed very low Li contamination level. First, the Li neutrals can be very easily ionized with ~5.4 eV of first ionization energy. The ionized Li particles tend to be screened by the magnetic field preventing further inward penetration. Secondly, the Li ions are very low recycling in nature that once Li ions or neutrals hit the wall, they tend to stick to the wall and not recycle back into the plasma. This low recycling nature of Li keeps the Li density in the plasma edge region very low which further reduces the probability of Li ions to enter the plasma core. The spectroscopic measurements of Li lines performed at the mid-plane indeed show very low Li edge density level even with the relatively large Li evaporation rates. Lastly, neoclassical transport calculations show that

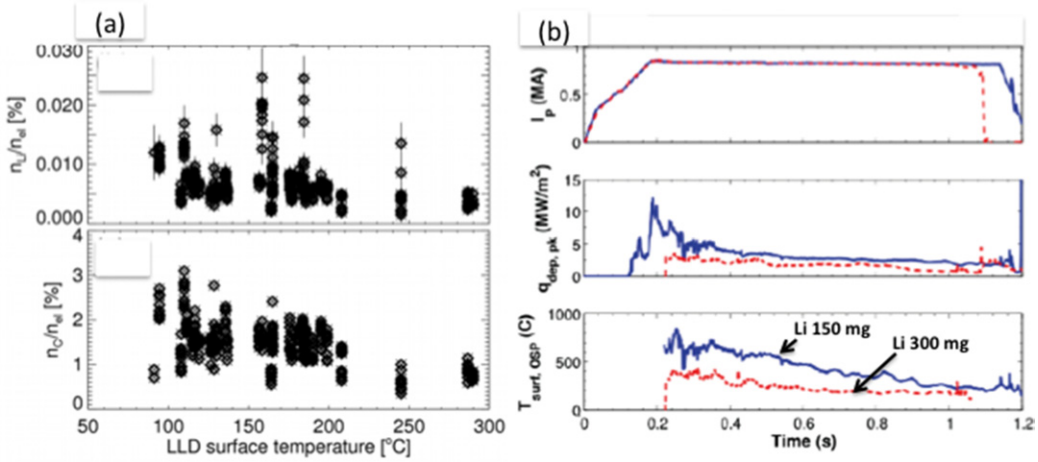

Figure 3. (*a*) Li and carbon dilution fractions as a function of the LLD surface temperature at $R = 135$–140 cm at $t = 500$–600 ms in NSTX. (*b*) Divertor surface temperature and corresponding heat flux as a function of Li evaporation for otherwise similar NBI heated H-mode discharges. Pre-discharge Li evaporation of 150 mg shown as blue solid lines and 300 mg as red dashed lines.

Li ions have an order of magnitude larger radial diffusivity compared to carbon ions making Li much less confined [33]. These properties make Li from the diverter chamber much less likely to enter and dilute the plasma core which makes Li highly desirable material for the divertor PFC application. It should be also pointed out that the routine use of Li in NSTX has essentially eliminated the need for conventional wall conditioning techniques such as helium glow-discharge-conditioning which took a longer time between shots than it did to apply enough lithium to achieve reproducible discharges. As a result, the lithium coating has significantly improved the plasma shot availability in NSTX (by up to 50% over the pre-Li plasma operations), resulting in a record number of plasma shots in a year [34].

A particularly important and relevant observation from the NSTX LLD experiment for the present paper is the divertor heat flux reduction accompanying the Li coating of divertor surfaces in NSTX [35]. As shown in figure 3(*b*), the measurements showed a ∼50% reduction in peak heat load on the divertor strike-point surfaces with only a modest amount of Li ∼300 mg evaporation prior to the discharge compared to 150 mg evaporation. The heat flux reduction is associated with an increase in the localized radiation measured by bolometers from the region above the inner and outer strike points. Interestingly, the radiation level is reduced in the divertor private flux region, which is not well understood at present [35]. The bolometric signal interpretation of the private flux region is complex since the private flux region is not magnetically connected to the active divetor heat flux regions. The reduced divertor heat flux through divertor bolometric radiation observed in the NSTX lithium divertor PFC coating experiment is consistent with the results from the previous theoretical model calculations of enhanced Li radiation and other Li experiments [36, 37]. The amount of Li coating on the divertor strike-point region in NSTX is a small fraction of evaporated Li. For example, it is estimated that less than 10% of the evaporated Li is deposited on the LLD surface [24]. In order to understand possible underlying process and explore future possibility, we performed a simple model calculation of Li radiative loss of a Li divertor as described in the next section.

3. A model calculation of lithium radiative divertor heat flux reduction

The divertor heat flux reduction observed in NSTX with a modest Li application suggests an interesting possibility of Li for handling the divertor heat flux. Since Li with low charge states is known to radiate relatively little in the coronal equilibrium limit, Li has not thus far been considered as an effective radiator in high temperature fusion plasmas. However, previous model calculations have shown that the Li radiation values can be significantly enhanced (2–3 orders of magnitude) over the coronal equilibrium values if the Li ions are poorly confined as expected in the plasma edge and in the divertor region [36, 37]. It should be noted that this radiative loss can greatly exceed the energy loss from the previously considered lithium evaporation [38] thus can significantly reduce the required LL needed for the divertor heat flux reduction. In figure 3 of [36], the non-coronal equilibrium Li radiation value per electron per Li particle which we term here I_{Li} is shown as a function of electron temperature T_e for 1–1000 eV for various values of $n_e\tau$ where n_e is the electron density and τ is the Li particle confinement time. The coronal equilibrium values are when $n_e\tau$ is infinity. The radiation level goes up as $n_e\tau$ decreases. This is because the lithium radiative loss cooling occurs mostly in the initial phase of lithium atom ionization process and it decreases as the lithium ion becomes fully ionized approaching the coronal equilibrium limit. For this reason, the lithium radiation loss becomes relatively insensitive to the electron temperature as the lithium plasma transit time become short compared to the coronal equilibrium time. Since the Li radiation level is highly dependent on the Li particle confinement time, it is instructive to examine Li particle transport as Li is injected from the divertor plate near the strike-point region along the magnetic field line. For a typical NSTX divertor plasma parameter, the ion–ion collisions are dominant collisional process and Li ions are expected to collide relatively rapidly with short mean-free-path lengths. For example, for $n_e \sim 1 \times 10^{13}$ cm^{-3} and $T_e \sim T_i$ of 10 eV, the doubly ionized Li has a mean free path of about 5 mm and very short collision time of

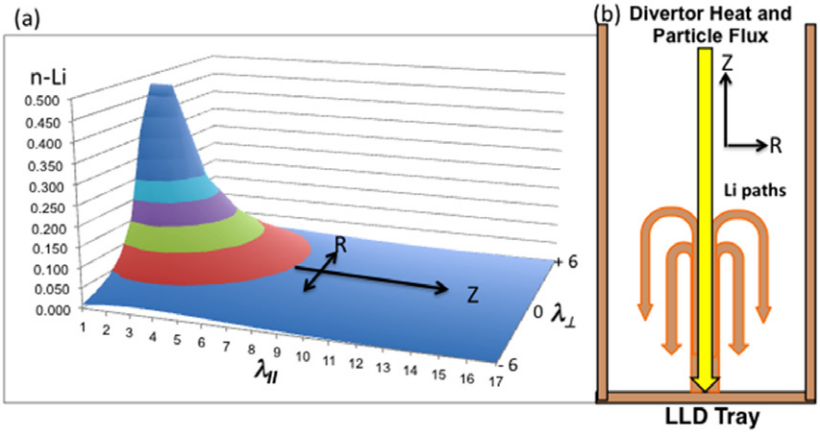

Figure 4. (*a*) Normalized Li particle density as a function of parallel (z) and perpendicular diffusion scale lengths. (*b*) Schematic of possible Li particle transport paths.

$\sim$1 μs. Based on the short collision time and mean-free-path length, the Li ion transport can be described by a 2D parallel and perpendicular diffusive model as shown in figure 4(*a*). Lithium atoms liberated from the divertor surface rapidly ionize and then travel along field lines while undergoing successive ionizations. The Li ions are also subject to cross-field diffusion which might be expected to approach the level of Bohm diffusion. As the particles diffuse radially, they continue to diffuse axially and a significant fraction of Li ions can come back to the divertor plate surfaces with some radial diffusion induced displacements as depicted in figure 4(*b*). The lithium ions are assumed to be lost once it reaches the LLD tray (horizontal surface) or the side walls (vertical surfaces). The net result is the Li is transported axially but due to radial diffusion, the injected Li is re-deposited back to the divertor plate surfaces but dispersed radially. From this model, we expect this movement of Li particles near the divertor plate to be quite rapid and the associated particle confinement time to be quite short as one would typically expect near the end plates of an open plasma system. An effective particle confinement time may be order of parallel transit time of lithium ions. It can be also reduced by charge-exchange and perpendicular diffusions. The transit time depends on the lithium ion energy and its distance from the divertor plate. For example, $\tau = 170\,\mu$s for a 4 eV lithium ion 5 cm away (i.e. $Z = 5$ cm) from the divertor plate and $\tau = 140\,\mu$s for a 50 eV lithium ion 23 cm away. Also as noted above, the charge exchange and anomalous perpendicular diffusion could reduce τ further. If we assume $\tau = 100\,\mu$s and $n_e \sim 10^{13}$ cm^{-3} or $n_e\tau \sim 10^9$, from [37], one obtains I_{Li} (*the Li radiation power per one atom and one electron*) $\sim(1\text{–}3) \times 10^{-26}$ W cm^3 for a relatively wide range of plasma temperature. We will therefore use $I_{Li} \sim 10^{-26}$ W cm^3 for this modelling calculation. Another interesting Li radiation characteristic to note is that Li radiated power per plasma volume $P_{Li} \propto I_{Li} n_e n_{Li} \propto n_e n_{Li}/\tau$ where n_{Li} is the lithium ion density. On the other hand, $n_{Li} \propto N_{Li}-\text{inj} \times \tau$ where $N_{Li} - \text{inj}$ is the lithium injection rate. One would then obtain $P_{Li} \propto n_e N_{Li} - \text{inj}$ which implies that the Li radiation level does not depend so sensitively on the actual Li confinement behaviour (τ) but more directly on $N_{Li} - \text{inj}$. As discussed above, in this relatively short particle confinement regime, the radiation level is determined by the number of lithium atoms entering the plasma not so much on how long the lithium ions are confined in the plasma since the radiation mainly takes place during the early ionization phase. So, the actual Li injection rate $N_{Li} - \text{inj}$ appears to be a robust quantity in determining the Li radiation level in the divertor. It should be also noted that though not fully accounted in this present radiation based model, the lithium atom injected into the plasma would consume a significant amount of energy (well over 100 eV per atom) through evaporation, ionization and thermalization (heating up by the plasma) processes in addition to the radiative, charge-exchange and diffusive processes.

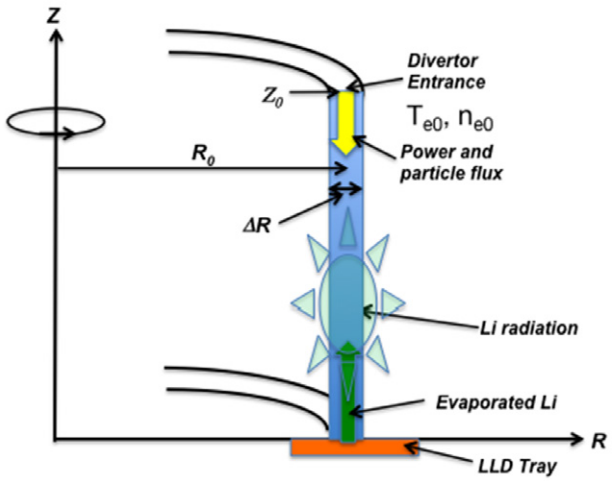

Figure 5. A schematic of RLLD modelling geometry.

In order to understand the NSTX lithium coated divertor observation, we carried out a simple model calculation to estimate the effect of Li radiation on the divertor heat flux using above Li radiation assumptions. To elucidate the lithium radiative cooling effect, we choose a simple cylindrical shell geometry with its radius to be the divertor strike position radial position R_0 with the shell width to be an effective divertor strike-point radial width ΔR with the vertical height Z_0 representing a nominal divertor vertical length as shown in figure 5. In this model, magnetic field and its pitch is assumed to be constant (where the toroidal displacement $R_0\Delta\phi$ is 20 times the vertical displacement ΔZ) and, therefore,

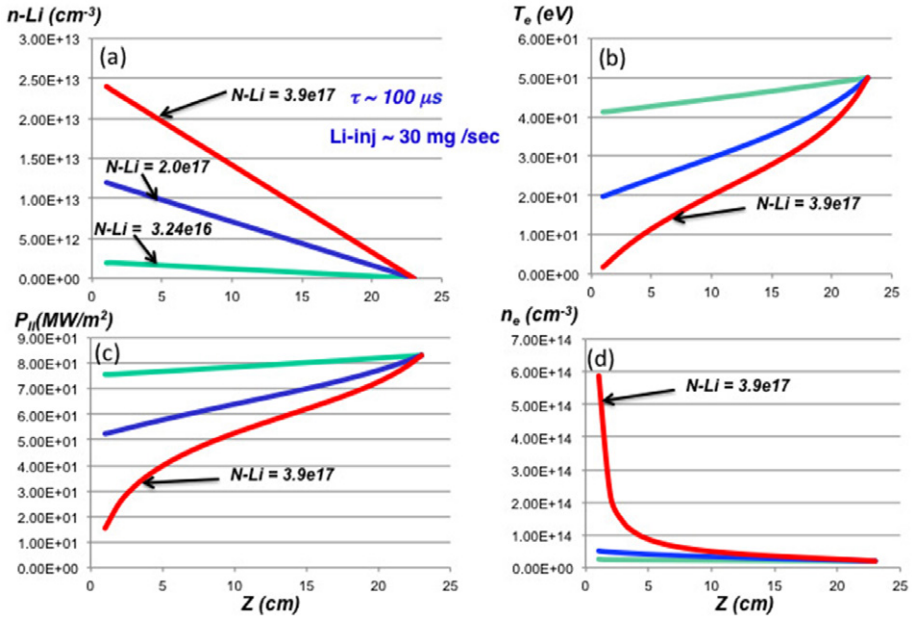

Figure 6. Calculated divertor heat flux reduction due to Li radiation in the NSTX LLD parameters. (*a*) Assume Li particle densities as labelled as a function of axial divertor distance. The total Li particles as labelled. (*b*) Electron temperature profile, (*c*) parallel power flux and (*d*) electron density profile for the corresponding Li density profiles. The divertor throat ($Z = 23$ cm) $T_e = 50$ eV and $n_e = 2 \times 10^{13}$ cm^{-3} were used in the model.

there is no flux expansion or other geometric effects within the divertor chamber. The divertor vertical region is divided into a number of cells (typically 23) and, within each cell, the plasma parameter changes due to the Li radiation are calculated using the conduction limited two-point model [39]. Here the radiation causes the volumetric loss of $q_{rad} = f_{power} q_0$ where q_0 is the incident heat flux into the cell. The force balance constraint within the cell leads to the reduction in the electron temperature in the cell of $\Delta T_{e0}/T_{e0} = 1 - (1 - f_{power})^2$ where T_{e0} is the electron temperature at the entrance of the cell. This model is a linear calculation therefore does not describe non-linear processes such as divertor detachment and plasma sheath effects. The plasma parameters at the divertor entrance are assumed to be the multi-point Thomson scattering (MPTS) temperature and density measured at the plasma mid-plane with $T_i = T_e$. For this model, we assume a given Li density profile, which is maximum at the Li divertor surface ($Z = 0$) and then decreases along the field line as the Z is increased and the lithium density vanishes at the divertor entrance at Z_0. We carried out calculations using three Li density profile types, linear $(1 - Z/Z_0)$, parabolic $[1 - (Z/Z_0)^{0.5}]$ and square $[1 - (Z/Z_0)^2]$ profiles. Interestingly with this present model calculation, the divertor heat flux reduction appears to depend mainly on the total amount of the Li ions in the divertor plasma, not very sensitively on the actual Li particle profiles. Therefore in this paper, we only show the linear Li profile model calculation results. It should be noted that our calculation assumes given lithium profiles which is then used to calculate the radiative loss. How to obtain such lithium profiles is to be determined. The lithium particle injection from the divertor strike point along the field line is perhaps the most natural way which can also be used to protect the divertor strike-point surfaces. That is the motivation of assuming lithium density profile to monotonically decrease from the divertor plate. If it is desirable to have the lithium population more upstream from the divertor plate, there are other ways to introduce lithium into the divertor plasma. For example, one can use a lithium powder injector [40] to inject lithium farther upstream from the divertor plate if desired. One can also envision a lithium 'spray' which can inject LL from the divertor side wall as needed. The active lithium injection from the divertor side wall has an advantage of relatively narrow divertor plasma channel (short distance) for lithium delivery and the injection can be made relatively well controlled. The active lithium injection can further help reduce the divertor head load through increased energy loss channels as noted above.

For the NSTX parameters, we assumed $R_0 = 75$ cm, $\Delta R = 3$ cm and $Z_0 = 23$ cm for three levels of Li particle density *n-Li* as a function of the diverter vertical position as shown in figure 6. The corresponding total number of lithium particles *N-Li* is indicated in figure 6(*a*). As shown in figure 6(*c*), the Li radiative cooling can reduce the diverter heat flux significantly with only *N-Li* $\sim 10^{17}$. The corresponding temperature and density profiles are shown in figures 6(*b*) and (*d*), respectively. The divertor Langmuir probe analysis of LLD discharges [41] (at $Z = 0$) shows $n_e \sim$ (3–5) $\times 10^{14}$ cm^{-3} and $T_e \sim$ 3–5 eV which is consistent with the modelling. Since the divertor heat flux to PFC is a factor of ~20 down from the parallel heat flux (due to the magnetic field line pitch in the divertor region), the observed 2 MW m^{-2} is consistent with the calculated 20–40 MW m^{-2} parallel heat flux. With 100 μs confinement time, the amount of injected Li is estimated to be 30 mg s^{-1} which is roughly in agreement with the NSTX experimental range. In terms of the lithium injection mechanisms, for relatively low divertor surface temperature of $\leqslant$400 °C, the sputtering is the main injection mechanism [42, 43]. The sputtering rate goes up with temperature and since it is mainly depending on the plasma

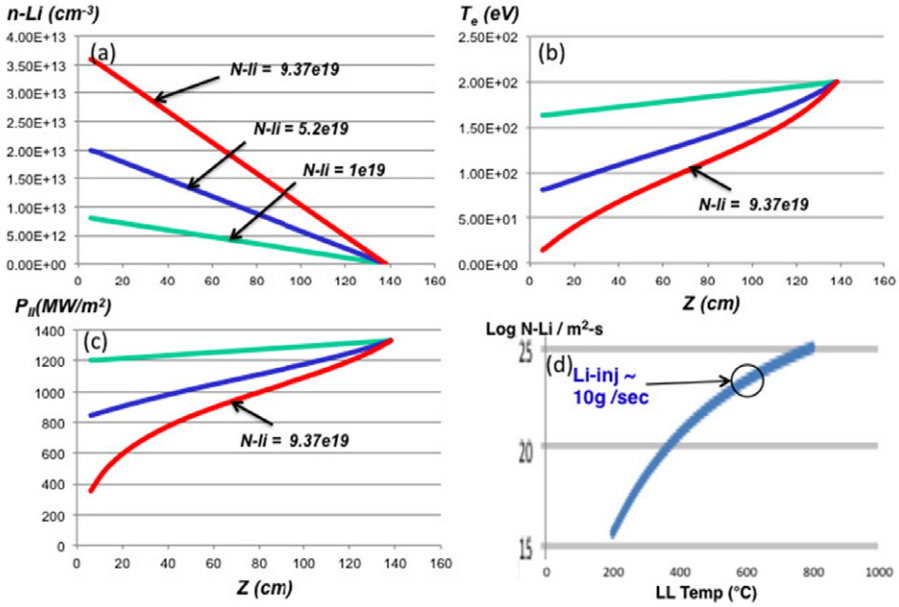

Figure 7. Calculated divertor heat flux reduction due to Li radiation in an ITER-size divertor parameters. (*a*) Assume Li particle densities as labelled as a function of axial divertor distance. The total Li particles as labelled. (*b*) Electron temperature profiles. (*c*) Parallel power flux for the corresponding Li density profiles. (*d*) Li evaporation rate per m^2 as a function of divertor temperature. The divertor throat ($Z = 138$ cm) $T_e = 200$ eV and $n_e = 4 \times 10^{13}$ cm^{-3} were used in the model.

potential, it can occur at larger divertor surface area. At higher temperature of $\geqslant$400 °C, the evaporation rapidly increases and becomes dominant particularly near the strike point when the temperature rise due to the heat flux becomes high [36].

A similar estimate for an ITER-size fusion power plant with $R = 6$ m, $\Delta R = 10$ cm, and $Z_0 = 132$ cm is shown in figure 7. The Li density profiles and corresponding parallel heat flux and temperature profiles are shown in figures 7(*a*)–(*c*), respectively. The amount of Li needed to reduce the divertor heat flux is naturally much larger than NSTX due to larger divertor size and higher heat flux, but it is still N-Li $\sim 10^{20}$ which is only a fraction of mg of Li ions in the divertor plasma. With $\tau = 100$ μs, the amount of required Li injection rate is ~ 10 g s^{-1} which is still relatively modest. It should be noted that this level of Li evaporation can be achieved if the LL surface temperature in the strike-point region goes up to ~600 °C as shown in figure 7(*d*). Since the vertical scale is logarithmic, a small amount of LL temperature rise could cause much higher evaporation rate and vice versa. If the desired heat flux reduction is not achieved, the divertor strike-point temperature would rise and thereby more lithium is injected into the divertor plasma which then facilitates further radiative cooling until an equilibrium is reached. So, the Li diverter surface has a self-regulating property of evaporating as much Li as needed to reduce the divertor heat flux to an acceptable value. One can also envision to control the Li particle injection rate by controlling the LL temperature if needed. It is therefore important to ensure an adequate amount of LL available at the location of intense heat flux (i.e., near the divertor strike point). The LL surface can also provide a 'sacrificial' surface to protect the substrate solid material even from transient high heat loads such as the ones caused by ELMs. If the transient heat flux is high, that much more Li would be evaporated and ionized, which would then increase the radiative cooling until an equilibrium condition is reached. For example, in an ITER scale tokamak reactor, with the enhanced radiative process, only a modest amount (~1 cm^3) of LL is estimated to be needed to radiate the expected heat pulse of ~10 MJ for an exceptionally large ELM event. This self-regulating, 'sacrificial' Li surface property is probably the reason for the Li coated NSTX divertor plate to be able to survive the high power divertor operation in NSTX without any sign of surface erosion nor damage [24].

4. RLLD concept

The ability for Li to radiate the divertor heat flux suggests a possibility of a Li-radiation-based LL divertor concept, which we term RLLD. Because of the low melting temperature of ~180 °C, Li naturally exists as liquid in a fusion reactor environment. Simplified schematics of the RLLD concept is shown in figures 8(*a*) and (*b*). The basic configuration is to place the RLLD at the bottom of the reactor chamber for an obvious reason of collecting LL. The RLLD configuration also has an additional advantage of capturing any loose micron size dust particles known to be generated via plasma wall interaction within the reactor chamber [44]. The dust generation in a reactor chamber is believed to be a serious tritium inventory and safety issue if it accumulates unchecked. As shown in figure 8(*b*), LL is introduced at the upper part of the RLLD at multiple toroidal locations and the LL flows down slowly due to gravity and spreads through capillary action into a thin film <1 mm thick on the RLLD side wall. The flow velocity is sufficiently slow so the MHD forces should be negligible as the LL accumulates at the bottom of the RLLD.

Because the RLLD side wall area is quite large (~100 m^2 for $R = 6$ m with diverter depth of 1.3 m), the Li coated wall

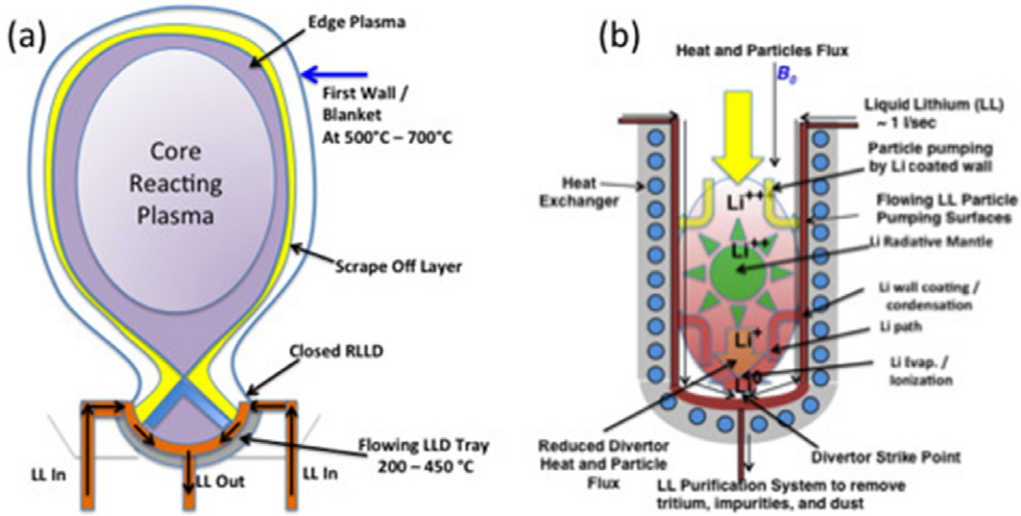

Figure 8. A possible RLLD configuration in a fusion power plant. (*a*) RLLD is envisioned to be placed at the bottom of the reactor chamber to capture LL, dust, and other solid impurities. (*b*) A simplified schematic of RLLD chamber. The LL flows down along the side wall to provide pumping and the thicker LL layer at the bottom provide a radiative Li source for heat flux reduction and divertor substrate protection.

acts as an efficient particle pump for the reactor chamber. As shown in figure 8(*b*), the RLLD side wall with heat exchanger also functions as the diverter heat removal system for the heat from the divertor Li radiation as discussed in section 3. The thin liquid layer results in large viscous forces in addition to MHD damping and the resulting flow velocities are expected to be small which enables the temperature transport to be described by thermal conduction [45]. The thin LL layer therefore insures the efficient heat transfer to the RLLD divertor wall substrate for the heat removal. There is also some concern on the control of the LL flow which may not be uniform [46]. This motivates the multiple toroidal locations of Li injection. But even if there are some non-uniformity of the LL flow, it might be still acceptable since the divertor side walls should experience relatively mild heat load so that the LL does not have to play the protective function as for the case of the divertor strike-point area. If a better LL flow uniformity is desired, it might be advantageous to apply porous coatings to enhance the capillary action as done on the NSTX LLD. Since the LL thin layer flow is slow, the Weber number ($We = \rho v^2 l/\sigma$, a measure of fluid flow inertia importance versus surface tension σ) is expected to be quite small that a finer flow uniformity control is probably not necessary. The LL then accumulates at the bottom of RLLD and forms a thicker LL layer perhaps $\sim$ few mm. The RLLD configuration is designed to have the divertor heat flux impinges on the LL surfaces at the bottom of RLLD. As described in section 3, Li is evaporated from the divertor strike-point surface due to the intense heat flux which raises the LL surface temperature to evaporate sufficient Li into the divertor plasma. The evaporated Li particles are quickly ionized by the plasma due to very low ionization energy and the ionized Li ions can move quickly into the divertor plasma along the magnetic field and provide a strongly radiative layer of plasma ('radiative mantle'), thus could significantly reduce the heat flux to the divertor strike-point surfaces, protecting the divertor surface. It is important to insure the availability of LL to protect the substrate solid material. For this reason, it might be advantageous to implement a mechanism to directly introduce LL to the strike-point region. An example of a possible divertor PFC is shown in figure 9 where LL reservoir replenishes the PFC surface through capillary action. An efficient heat removal by a compressed helium (He) or a supercritical carbon dioxide (s-CO_2) gaseous cooling using the US-based T-tube concept [47] may be considered. In addition to dust capture and chemically based Li pumping, RLLD may be also used to capture the fusion alpha particles (He) which is expected to be trapped in LL [48]. The accumulated LL at the bottom of RLLD with impurities and dust particles is transported to outside of reactor chamber, and purified through a close-loop LL system as described in the next section.

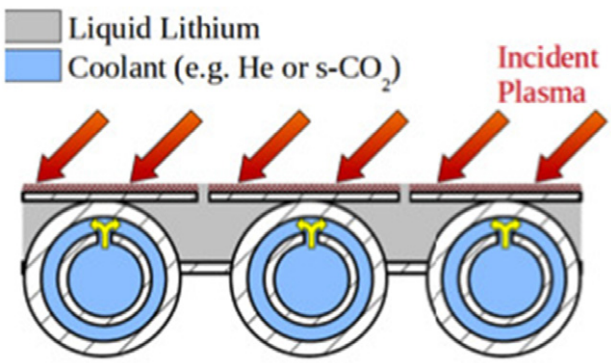

Figure 9. Conceptual diagram for an actively cooled, actively wetted liquid Li PFC.

LL purification loop for RLLD. For RLLD to be viable for steady-state reactor operations, it is essential to continually purify the LL by removing D, T, He, and other impurities including the Li compounds and dust as depicted in figure 10. Prompt removal of tritium is particularly important to keep the tritium inventory level low. Fortunately, the LL circulation

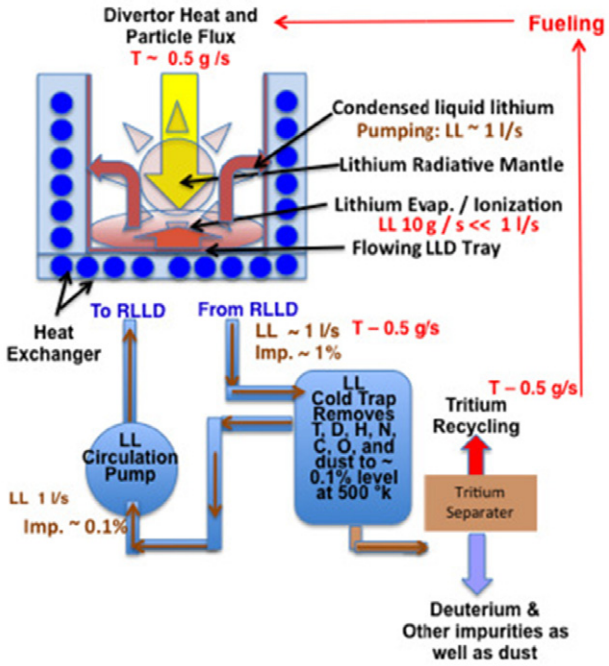

Figure 10. A schematic for the LL purification loop for RLLD in a power plant.

requirements for purification is relatively modest. For a 1 GW-electric power plant, the main 'impurity species' would be the hydrogenic (D–T) fuel gas and it is estimated that about 0.5 g s^{-1} of tritium gas is used as only 1% of which is actually burned through D–T fusion reaction. Since 99% of the tritium must be recycled and it is highly likely to be trapped within LL by forming such Li compounds as Li–T, the LL circulating loop must carry ~0.5 g s^{-1} of tritium out of the reactor vacuum chamber. If one were to require LL to contain only 1% of impurities to insure good LL flow property, about 1 l s^{-1} of LL-loop capacity might be sufficient to bring the generated impurities out of the reactor vessel. In this case, 1 l of LL also contains ~0.5 g of tritium. At this high concentration level, it is relatively easy to extract tritium by the cold trap technology being develop by the International Fusion Materials Irradiation Facility (IFMIF) [49]. In this technique, the tritium and other impurities can be extracted to about 0.1% level. There are techniques to further remove tritium [50] but 0.1% level purification may be quite satisfactory for the RLLD system. In terms of the tritium inventory, even if the RLLD LL-loop system contains 10001 of LL, the total tritium inventory is still only 500 g which should be acceptable from the tritium inventory point of view [51]. As noted previously, such a loop system can also bring out the dust generated within the reactor chamber and also can be used to capture and remove He (alpha particles) as well.

Compatibility of RLLD with reactor hot first wall. As shown in figure 8(*a*), it is generally envisioned in magnetic fusion reactor studies that the reactor first wall temperature will be high (~600–700 °C) to keep the first wall surface relatively clean, particularly of tritium to keep the tritium inventory reasonably low, and to achieve high electrical power conversion efficiencies. On the other hand, the RLLD temperature (except for the strike-point region where the temperature could be higher) is likely to be in the ~200–450 °C range to avoid excessive Li evaporation [36] (see also figure 7(*d*)). Because of this operating temperature difference, LL is often thought to be not compatible with the reactor environment. However, the lower operating temperature of LL may in fact make it more suitable for the reactor divertor operation. For RLLD operating well below the first wall temperature, the Li and associated impurities should migrate towards the lower temperature RLLD chamber, and keep the higher temperature first wall relatively clean. There was an interesting experiment in T11-M where a lower operating temperature capillary-porous system (CPS) was able to actually collect Li from the higher temperature CPS via plasma interactions [17]. The purpose of the experiment was to demonstrate how the Li particles could migrate towards the lower temperature region within a fusion plasma chamber. The approach would be similar to a dehumidifier (which has colder condensing surfaces) collecting the water vapour within the room. In addition, all plasma particles tend to end up in the divertor chamber because of the net particle flow from the main chamber to the closed divertor chamber with frictional forces in the direction of the closed strongly pumping divertor chamber. Therefore, a RLLD operating below the first wall temperature, together with a purifying system as shown in figure 10, could serve as the gas pumping, tritium recovery, and impurity control system for the entire reactor chamber. Also importantly, with lower operating temperature, one can envision utilizing steel-based alloys as potential substrates and support structures of RLLD where the LL provides a low-Z protective layer over the high-Z steel. This material choice eliminates the need to transition from structural steels to tungsten where the operating temperature windows do not always overlap [52].

Applicability of lithium in magnetic fusion reactors. At the second Lithium Symposium in 2011 [21], a panel discussion was held addressing the previously identified questions at the first Lithium Symposium [20], 'Is a Li PFC viable in magnetic fusion reactors such as ITER?' The following specific technical issues for Li reactor applications were discussed: (1) handling high divertor heat flux, (2) removal of deuterium, tritium, and impurities from LL, (3) removal of high steady-state heat flux from divertor, (4) flowing of LL in magnetic fields, (5) longer term corrosion of internal components by LL, (6) safety of flowing LL and (7) compatibility with LL with a hot reactor first wall. In this paper, we have attempted to address many of those issues for the RLLD applicability at the conceptual level: the divertor heat flux handing prospect of RLLD (issue #1) was addressed in section 3. Removal of deuterium, tritium, and impurities from LL (issue #2) was covered in section 4. For the issue #3 of removal of high steady-state heat flux from divertor RLLD, since the divertor heat load is dispersed over the large divertor wall surfaces through radiation, the divertor heat load can be removed through secondary divertor structures with heat exchanger (as shown in figures 8(*b*) and 9). Such structures can be cooled, for example, by circulating high-pressure He gas system or s-CO_2 system [47] which is considered a relatively safe approach for LL. Regarding the issue #4 of flowing of LL in magnetic fields, because of the relatively low circulating

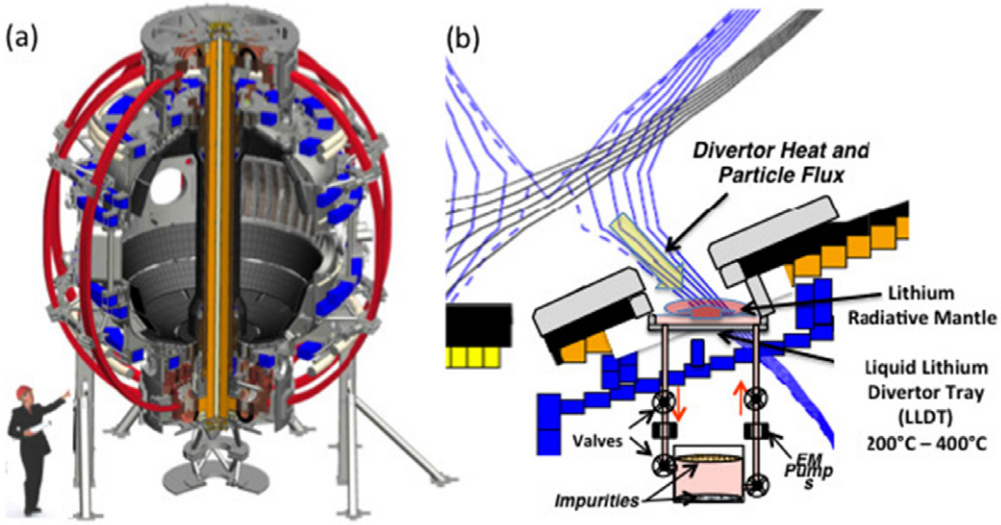

Figure 11. (*a*) A schematic for the NSTX-U device. (*b*) A possible prototype RLLD system on NSTX-U.

LL volume ($\sim 1\,\mathrm{l\,s^{-1}}$) of circulation of RLLD, the required power is modest for the LL circulation. In addition, the RLLD concept relies mainly on the slow LL flow via gravity and capillary action along the RLLD wall so that the magnetic field induced forces on LL should be negligible. The issues #5 and #6 of longer term corrosion and safety issues are well defined material science and safety engineering issues. The relatively low operating temperature range of RLLD and its associated LL-loop system should be advantageous from corrosion and safety point of view. The low operating temperature also makes available broader choices of iron based alloy material. It should be also noted that those engineering issues are being addressed in the R&D activities for the IFMIF [49] and fusion blanket module development. Finally the compatibility of RLLD with a hot reactor first wall (issue #7) was addressed in section 4

5. Discussions and conclusions

The application of Li coating on divertor PFCs in NSTX has produced significant improvements in H-mode plasma confinement and performance. The resulting broadened plasma pressure profile is advantageous for high beta stability which is important for achieving high performance H-mode operation for tokamak reactors. It is also noted that even with significant application of Li on PFCs (e.g., up to 1300 g of Li was evaporated into NSTX during the 2010 campaign), no adverse effects on plasma operations were evident. Indeed, very little contamination (<0.05%) of Li in the main fusion plasma core was observed in the H-mode plasmas. An important observation in NSTX particularly relevant for the present paper is that the application of modest amount of Li coating on divertor surfaces has resulted in more than 50% reduction in the peak divertor heat flux.

Based on the NSTX Li experimental results, we proposed a radiative cooling based LL divertor concept (RLLD) with an aim for solving the highly challenging divertor heat load problem for fusion reactors (figure 8). Because of the low melting temperature of $\sim 180\,^{\circ}\mathrm{C}$, Li naturally exists as liquid in a fusion reactor environment. The RLLD is placed at the bottom of the reactor chamber for an obvious reason from the LL handling point of view and also to capture any impurity particles including dust generated within the reactor chamber. The LL is introduced at the upper part of the RLLD at multiple toroidal locations and it gradually flows down the RLLD side wall as a thin film via gravity and capillary action. The thin LL film thus formed should provide very effective pumping for working gas, impurities, and dust within the reactor chamber. The RLLD chamber being the lowest temperature in the reactor chamber should facilitate the pumping action for the entire reactor chamber. The LL accumulates at the bottom of RLLD where the divertor strike point is placed. By placing LL surface in the path of the divertor strike point, the LL is evaporated from the surface. The evaporated Li is quickly ionized by the plasma and the ionized Li ions can radiate strongly, reducing the heat flux to the divertor strike-point surfaces and protecting the substrate material. NSTX-U [8, 54] can provide very high divertor heat flux to the PFC ($\sim$40–60 $\mathrm{MW\,m^{-2}}$), comparable to that is expected in future tokamak reactors such as FNSF and DEMO. A conceptual RLLD prototype system could be tested in NSTX-U as shown in figure 11(*b*) [55]. Finally, it should be emphasized that Li PFC applications are quite flexible and diverse. There are other divertor configurations that could greatly reduce the heat flux at the divertor strike point through expanding the divertor flux lines [56, 57]. RLLD application should be quite compatible with various divertor geometry and magnetic confinement configurations providing the same benefits of Li. Application of the RLLD concept may also be considered for protecting the tungsten-based solid divertor PFC surfaces such as the ones for ITER, as long as a way to purify or refresh Li surfaces can be provided. In summary, a radiative mantle based LL divertor solution (RLLD) provides the exciting prospect of combining a means to improve fusion reactor performance with a practical solution to the highly challenging divertor heat handling issue confronting magnetic fusion reactors.

Acknowledgment

This work was supported by DoE Contract No DE-AC02-09CH11466.

References

[1] ReNeW is a planning activity of the US DOE Office of Fusion Energy Science (OFES) 2009 *Magnetic Fusion Energy Science Research Needs Workshop Report* http://burningplasma.org/web/ReNeW/ReNeW.report.web2.pdf
[2] ITER Physics Basis Expert Groups on Confinement and Transport and Confinement Modelling and Database, ITER Physics Basis Editors 1999 *Nucl. Fusion* **39** 2175
[3] Nygren R.E. *et al* 2011 *J. Nucl. Mater.* **417** 451
[4] Tobita K. *et al* 2009 *Nucl. Fusion* **49** 075029
[5] Visca E. *et al* 2012 *Fusion Eng. Des.* **87** 941
[6] Wang X.R. *et al* 2012 *Fusion Eng. Des.* **87** 732
[7] Peng Y.-K.M. *et al* 2009 *Fusion Sci. Technol.* **56** 957
[8] Menard J.E. *et al* 2012 *Nucl. Fusion* **52** 083015
[9] Mansfield D.K. *et al* 2001 *Nucl. Fusion* **41** 1823
[10] Abdou M.A and the APEX Team *et al* 2001 *Fusion Eng. Des.* **54** 181
[11] Majeski R. *et al* 2006 *Phys. Rev. Lett.* **97** 075002
[12] Hirooka Y. *et al* 2009 *J. Nucl. Mater.* **390–391** 502
[13] Hu J.S. *et al* 2010 *Fusion Eng. Des.* **85** 930
[14] Xu G.S. 2011 *Nucl. Fusion* **51** 072001
[15] Mazzitelli G. *et al* 2010 *Fusion Eng. Des.* **85** 896
[16] Kugel H.W. *et al* 2010 *Fusion Eng. Des.* **85** 865
[17] Mirnov S.V. *et al* 2012 *Fusion Eng. Des.* **87** 1747
[18] Tabarés F.L. *et al* 2008 *Plasma Phys. Control. Fusion* **50** 124051
[19] Munaretto S. *et al* 2012 *Nucl. Fusion* **52** 023012
[20] Hirooka Y. *et al* 2010 *Nucl. Fusion* **50** 077001
[21] Ono M. *et al* 2012 *Nucl. Fusion* **52** 037001
[22] Ono M. *et al* 2000 *Nucl. Fusion* **40** 557
[23] Kugel H.W. *et al* 2008 *Phys. Plasmas* **15** 056118
[24] Kugel H.W. *et al* 2012 *Fusion Eng. Des.* **87** 1724
[25] Bell M.G. *et al* 2009 *Plasma Phys. Control. Fusion* **51** 124054
[26] Maingi R. *et al* 2009 *Phys. Rev. Lett.* **103** 075001
[27] Maingi R. *et al* 2011 *Nucl. Fusion* **52** 1823
[28] Kaye S.M. *et al* 2013 *Nucl. Fusion* **53** 063005
[29] Guttenfelder W. *et al* 2012 *Phys. Plasmas* **19** 056119
[30] Kaye S.M. *et al* 2012 *Nucl. Fusion* **51** 113019
[31] Maingi R. *et al* 2010 *Phys. Rev. Lett.* **105** 135004
[32] Podesta M. *et al* 2012 *Nucl. Fusion* **52** 033008
[33] Scotti F. *et al* 2013 *Nucl. Fusion* **53** 083001
[34] Ono M. *et al* 2010 *Fusion Eng. Des.* **85** 882
[35] Gray T.K. *et al* 2013 The effects of increasing lithium deposition on the power exhaust channel in NSTX *Nucl. Fusion* submitted
[36] Rognlien T.D. and Rensink M.E. 2002 *Phys. Plasmas* **9** 2120
[37] Mirnov S.V. *et al* 2006 *Plasma Phys. Control. Fusion* **48** 821
[38] Nagayama Y. *et al* 2009 *Fusion Eng. Des.* **84** 1380
[39] Stangeby P.C. 2002 *The Plasma Boundary of Magnetic Fusion Devices* (Bristol: Institute of Physics Publishing)
[40] Mansfield D. *et al* 2010 *Fusion Eng. Des.* **85** 890
[41] Jaworski M.A. *et al* 2013 *J. Nucl. Matter* **438** S384
[42] Allain J.P. and Brooks J.N. 2001 *Nucl. Fusion* **51** 023002
[43] Doerner R.P. 2001 *J. Nucl. Matter* **290–293** 166
[44] Skinner C.H. *et al* 2010 *Rev. Sci. Instrum* **81** 10E102
[45] Jaworski M.A. *et al* 2009 *J. Nucl. Mater.* **390–391** 1055
[46] Hirooka Y. 2012 private communication, National Institute for Fusion Science, Japan, November 2012
[47] Dostal V., Driscol M.J. and Hejzlar P. 2004 A supercritical carbon dioxide cycle for next generation nuclear reactors *Technical Report* MIT-ANP-TR-100, MIT, March 2004 stuff.mit.edu/afs/athena/course/22/22.33/OldFiles/www/dostal.pdf
[48] Nieto M. *et al* 2006 *J. Nucl. Mater.* **350** 101
[49] Kondo H. *et al* 2011 *Fusion Eng. Des.* **86** 2437
[50] Katekari K *et al* 2012 *J. Energy Power Eng.* **6** 900
[51] Nishikawa M. 2011 *Fusion Sci. Technol.* **59** 350
[52] Zinkle S.J. and Ghoniem N.M. 2000 *Fusion Eng. Des.* **51** 55
[53] Kondo H. *et al* 2012 *Fusion Eng. Des.* **87** 418
[54] Gray T. *et al* 2011 *J. Nucl. Matter* **415** S360
[55] Ono M. *et al* 2011 *Fusion Eng. Des.* **87** 1770
[56] Soukhanovskii V.A. *et al* 2011 *Nucl. Fusion* **51** 012001
[57] Valanju P.M. *et al* 2009 *Phys. Plasmas* **16** 056110